J. Biochem. 123, 752-759 (1998)

Fluorescence Microscopic Demonstration of Cathepsin K Activity as the Major Lysosomal Cysteine Proteinase in Osteoclasts

Takeshi Kamiya,* Yasuhiro Kobayashi,† Kazuhiro Kanaoka,† Tomoki Nakashima,‡ Yuzo Kato,§ Akio Mizuno,* and Hideaki Sakai§,¹

*Department of Oral and Maxillofacial Surgery, †Department of Orthodontics, and §Department of Pharmacology, Nagasaki University School of Dentistry, 1-7-1 Sakamoto, Nagasaki 852-8588; and ‡Department of Hospital Pharmacy, Nagasaki University School of Medicine, Nagasaki 852-8523

Received for publication, November 14, 1997

The enzyme activity of lysosomal cysteine proteinases in vital rabbit osteoclasts and mouse osteoclast-like cells was visualized with Z-Leu-Arg-4-methoxy-β-naphthylamide (Z-LR-MNA) as the enzyme substrate. The MNA liberated by proteolysis forms a fluorescent insoluble Schiff-base product in the presence of 5-nitrosalicylaldehyde. Many small fluorescent particles, endproducts of the Z-LR-MNA hydrolysis, were observed in proximity to the bone surface underneath the actively resorbing osteoclasts, as well as in the cytoplasm. The Z-LR-MNA hydrolase activity was markedly diminished by bafilomycin A1 and chloroquine treatment. Moreover, the activity was completely inhibited by cysteine proteinase inhibitors such as leupeptin and E-64d, but not by other classes of proteinase inhibitors. About 60% of the hydrolase activity in mouse osteoclast-like cells was immunoabsorbed by anti-cathepsin K antibody-coupled Sepharose CL-4B beads, and about 10% of the activity was absorbed with the anti-cathepsin L antibody-coupled beads. Thus, the majority of the Z-LR-MNA hydrolase activity in osteoclasts was derived from cathepsin K. In contrast, using the same substrate in the assay, no detectable cathepsin K activity was observed in mouse peritoneal macrophages. The abundant cathepsin K activity in osteoclasts would therefore indicate a significant role of this enzyme in bone matrix degradation.

Key words: activity staining, cathepsin K, cysteine proteinase, osteoclast.

Active osteoclasts secrete protons that dissolve hydroxyapatite crystal into resorption lacunae. Under such an acidified condition, the lysosomal cysteine proteinases produced by osteoclasts have maximum activities and are thought to play important roles in the degradation of bone matrix proteins (*1, 2*). Indeed, inhibitors of cysteine proteinases significantly attenuate the bone resorption both *in vivo* and *in vitro* (*3-8*). Cathepsins B, K, L, H, and S have been identified as the major cysteine proteinases in osteoclasts. Accumulation of cathepsins B, K, and L in bone resorption lacunae has been demonstrated by immunohistochemical studies (*9-11,22*). Among these cysteine proteinases, cathepsin K is known to be osteoclast-specific and most abundantly expressed in the cell compared with other cathepsins (*12-19*). Moreover, cathepsin K has strong potency in digesting native collagen fibers (*20*). Application of antisense oligonucleotide to reduce translation of cathepsin K diminished the bone resorption activity of osteoclasts (*21*). Thus, cathepsin K seems to be the proteinase most active in proteolysis in the osteoclastic bone resorption.

Visualization of the proteinase activity with a histochemical method would be valuable in research on cathepsin K and on the development of inhibitors. The method would allow single-cell analysis of the enzyme activity without isolating osteoclasts from a mixed cell population. Herein, we present such a method. The activity of lysosomal cysteine proteinases in osteoclasts was visualized by using peptide derivatives coupled with 4-methoxy-β-naphthylamide (MNA) as the enzyme substrate. The endproduct of the proteolysis, free MNA, forms an insoluble fluorescent Schiff-base product in the presence of 5-nitrosalicylaldehyde. Thereby, the site of the proteolysis can be visualized by the fluorescent product.

MATERIALS AND METHODS

Materials—Z-Leu-Arg-4-methoxy-β-naphthylamide (Z-LR-MNA) was purchased from Enzyme Systems Products (Dublin, CA, USA). Z-Leu-Arg-4-methylcoumaryl-7-amide (Z-LR-MCA) was obtained from Peptide Institute (Osaka). 5-Nitrosalicylaldehyde (NSA) and keyhole limpet hemocyanin (KLH) were purchased from Katayama Chemical Industries (Osaka) and Sigma (St. Louis, MO, USA) respectively. Actinase E and collagenase (type 3) were obtained from Kaken Pharmaceutical and Worthington Biochemical (Freehold, NJ, USA), respectively. All the other reagents were of analytical grade.

Preparation of Osteoclasts—Rabbit osteoclasts were

¹ To whom correspondence should be addressed. E-mail: h-sakai@net.nagasaki-u.ac.jp

Abbreviations: PBS, phosphate-buffered saline; SDS-PAGE, sodium dodecyl sulfate-polyacrylamide gel electrophoresis; Z-LR-MNA, Z-Leu-Arg-4-methoxy-β-naphthylamide; NSA, 5-nitrosalicylaldehyde; FCS, fetal calf serum; MCA, 4-methylcoumaryl-7-amide.

prepared from rabbit (New Zealand White, 10 days old) long bones essentially according to the method of Kakudo *et al.* (*40*). The unfractionated bone cells were seeded on a collagen gel. Stromal cells were removed from the gel by enzyme digestion with 0.001% actinase E and 0.01% collagenase, followed by repeated washing with phosphate-buffered saline (PBS). Adherent cells, enriched in osteoclasts, were then detached from the gel with 0.1% collagenase treatment and used for the vital fluorescence staining. For preparation of osteoclast lysate, the unfractionated rabbit bone cells were plated on a plastic dish. The osteoclasts were concentrated by removing stromal cells with 0.001% actinase E treatment as described by Tezuka *et al.* (*23*). Mouse osteoclast-like cells were prepared by using the mouse co-culture system with calvaria-derived osteoblastic stromal cells and bone marrow cells according to the method described by Takahashi *et al.* (*24*). We used new born and 8-week-old ddY mice for the cell preparation. The osteoclast-like cells were concentrated by detaching the stromal cells from the plate with 0.001% actinase E treatment.

Vital Fluorescence Staining—The osteoclasts were cultured on dentine disks for 6 h in α minimum essential medium (αMEM) containing 10% fetal calf serum (FCS). The cells were then incubated with 0.5 mM Z-LR-MNA/15 mM 5-nitrosalicylaldehyde (NSA)/1 mM dithiothreitol (DTT)/0.5 mM EDTA/20 mM sodium phosphate (pH 7.0). After 45-min incubation at 37°C, the cells were fixed with 4% paraformaldehyde in PBS for 30 min at 4°C. The cells were further treated with 0.2% Triton X-100/PBS for 15 min at room temperature (RT) and stained with TRITC-phalloidin (1 μg/ml in PBS) for 1 h at 37°C. Cell nuclei were stained with Hoechst 33258 (1 μg/ml in PBS) for 5 min at RT.

In some experiments, cells were further stained for tartrate-resistant acid phosphatase (TRAPase) activity as described by Hashimoto *et al.* (*25*). The cells were examined with a fluorescence microscope (Axiophoto, Zeiss, Oberkochen, Germany) using the following filters: UV filter sets (excitation band pass filter, G365/emission band pass filter, LP420); Blue filter sets (BP450-490/LP520); and Green filter sets (BP530-585/LP615). The cells were also examined with a confocal laser scanning microscope (LSM-GB200, Olympus, Tokyo) set for Ar-laser excitation at 488 nm with the combination of the two long band pass filter sets (BP490/O515 and BP545/O590).

Effect of pH on Z-LR-MCA Hydrolase Activity—Cells were lyzed in buffer A (1% NP-40/140 mM NaCl/1 mM EDTA/0.5 mM cysteine/50 mM sodium phosphate, pH 6.0). The supernatant, after centrifugation at 15,000 × *g* for 30 min, was incubated with 5 mM Z-LR-MCA/1 mM cysteine/1 mM EDTA in one of the following buffers: 100 mM citrate buffer (range pH 2.0-5.0), 100 mM sodium phosphate buffer (range pH 5.5-8.0), or 100 mM Tris-HCl buffer (range pH 8.5-10.0). After a 40-min incubation at 37°C, the reaction was stopped with 3 volumes of 10 mM iodoacetic acid. The amount of liberated 4-methylcoumaryl-7-amide (MCA) in the solution was measured with excitation at 380 nm and emission at 460 nm. One unit (U) of the enzymatic activity was defined as the amount of enzyme releasing 1 pmol of MCA in 1 min.

Antibody Preparation—For the production of peptide antibodies against the mouse cathepsin K-C-terminal (CK-C) peptide and mouse cathepsin L-C-terminal (CL-C) peptide, an automated solid-phase peptide synthesizer (Applied Biosystems, model 430A) was employed to synthesize the following peptides (shown in single amino acid code):

$$\text{CK-C peptide} \quad \overset{+318}{\text{NH}_2}\text{-CGITNMASFPK}\overset{+329}{\text{M}}\text{-COOH}$$

$$\text{CL-C peptide} \quad \overset{+322}{\text{NH}_2}\text{-CGLATAASYPVV}\overset{+333}{\text{N}}\text{-COOH}$$

The sequence reported by Gelb *et al.* (*18*) was used for construction of cathepsin K peptides, and that described by Joseph *et al.* (*26*) for cathepsin L peptide. Each peptide was coupled to KLH with *m*-maleimidobenzoyl-*n*-hydroxysuccinimide ester (MBS, Pierce, Cambridge, UK) according to the method of Yoshimori *et al.* (*27*). New Zealand white rabbits were injected subcutaneously with 250 μg of each peptide-KLH conjugate, which was emulsified in Freund's complete adjuvant (Difco Laboratories, Detroit, MI). Booster injections were given 4 times at 4-week intervals, and the rabbits were bled from the ear 1 week after the last injection. The IgG fraction from the pooled sera was prepared with a HiTrap Protein A column (Pharmacia, Piscataway, NJ, USA).

Immunoabsorption and Immunoblotting—Each normal rabbit IgG, anti-cathepsin K-C terminal peptide (anti-CK-C) IgG, or anti-cathepsin L-C terminal peptide (anti-CL-C) IgG was coupled with CNBr-activated Sepharose CL-4B beads (Pharmacia). For reduction of non-specific adhesion of protein, the beads were pre-incubated with 5% FCS/ 3% bovine serum albumin in PBS for 1 h at 4°C and resuspended in buffer B (20 mM sodium phosphate buffer/ 0.5 mM cysteine/1 mM EDTA/140 mM NaCl, pH 7.0). Fifty microliters of the cell extract of mouse osteoclast-like cells was mixed with 250 μl of the IgG-coupled beads slurry (90% Sepharose suspension) in a small column. After gentle agitation for 8 h at 4°C, the solution was flushed from the column by centrifugation at 1,000 rpm for 3 min (RD-15, Hitachi, Tokyo) and washed twice with 100 μl of buffer B. All the flow-through fraction was collected, and the Z-LR-MCA hydrolase activity in the solution was assayed at pH 6.0 as described above. Adsorbed protein on the beads was eluted with 200 μl of 3 M sodium thiocyanate at pH 7.5.

Mouse peritoneal macrophages were isolated from aged female mice (BALB/c). The peritoneal space of each mouse was rinsed with warmed 0.9% NaCl, and the released cells were plated on a plastic plate. After 30-min incubation in 10% FCS containing RPMI 1640 medium, attached cells (more than 90% were macrophages) were collected and lyzed in buffer A. The supernatant was subjected to the immunoabsorption with the same procedure as employed for the samples of osteoclasts.

For immunoblotting, the proteins in the flow-through and adsorbed fractions were sedimented by mixing with 2 volumes of 100% saturated ammonium sulfate solution for 1 h on ice. After centrifugation at 15,000 × *g* for 30 min, the precipitated proteins were resuspended and denatured in sodium dodecyl sulfate (SDS)-solubilizing buffer (2% SDS, 100 mM DTT, 10% glycerol/0.0025% bromophenol blue in 62.5 mM Tris-HCl, pH 6.8). The samples were separated by means of 10% SDS-polyacrylamide gel electrophoresis and transferred onto a nitrocellulose membrane. The blotted membranes were immunostained with anti-CK-C

IgG or anti-CL-C IgG as described previously (*25*). The antigenic sites were detected with an ECL kit (Amersham, Buckinghamshire, UK). For verification of the specificity, anti-CK-C IgG and anti-CL-C IgG were preincubated with an excess amount of synthetic CK-C or CL-C peptide, respectively, and used for the immunoblotting. The intensity of the bands was quantified with an Image Master 2-D scanning densitometer (Pharmacia Biotech, Tokyo).

Others—Protein concentration was determined by the method of Lowry *et al.* (*28*).

RESULTS

Characteristics of MNA Substrate—When MNA (final concentration, 10 mM) was dissolved in 50 mM sodium phosphate buffer (pH 6.0) containing 100 mM NSA, it formed a Schiff-base product (Fig. 1A). Free MNA showed blue fluorescence under microscopic observation with UV filter sets, but no fluorescence under observation with Blue or Green filter sets (Fig. 1B, a-c). The NSA-coupled MNA formed insoluble needle-like fluorescent crystals after 30-min incubation at room temperature. The crystal showed yellow, green and red fluorescence under microscopic observation with UV, Blue and Green filter sets, respectively (Fig. 1B, d-f).

Z-LR-MNA Hydrolase Activity in Osteoclasts—Rabbit bone cells rich in osteoclasts were plated on dentine disks and stained with 0.5 mM Z-LR-MNA in the presence of 15 mM NSA at pH 7.0. The Z-LR-MNA hydrolase activities were visually detected as small yellow fluorescent particles, the product of NSA-coupled MNA. As demonstrated in Fig. 2a, multinuclear cells showed abundant yellow fluorescent particles under microscopic observation with the UV filter sets, while mononuclear cells showed few such particles. Most of the multinuclear cells were TRAPase-positive (Fig. 2b), strongly suggesting that they were osteoclasts. Mouse osteoclast-like cells plated on a dentine disk also showed abundant Z-LR-MNA hydrolase activity (Fig. 2c).

To ascertain the enzymatic properties of the Z-LR-MNA hydrolase, we tested the effects of various membrane-permeable reagents on the activity by comparison with the control activity (Fig. 3a). Bafilomycin A1, an inhibitor of vacuolar-type H^+-ATPase (>1 μM), and chloroquine (>10 μM), a lysosomotropic amine, effectively diminished the Z-LR-MNA hydrolase activity (Fig. 3, b and c). Cysteine proteinase inhibitors such as leupeptin (>1 μM) and E-64-d (>1 μM) also inhibited the activity (Fig. 3, d and e),

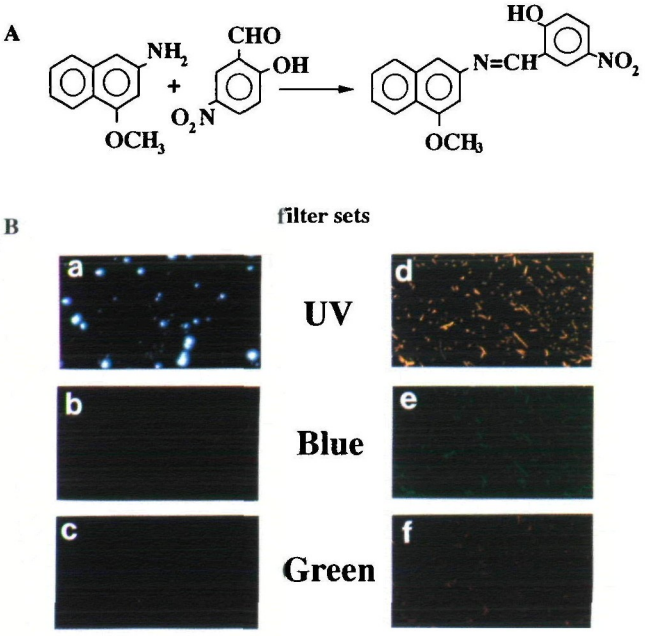

Fig. 1. Characteristics of 4-methoxy-2-naphthylamide (MNA) substrate. A: The reaction of MNA and NSA to form a Schiff-base complex. B: Fluorescence analyses of MNA (a-c) and NSA-coupled MNA (d-f) by means of fluorescence microscopy. Samples were examined with a fluorescence microscope with UV (a, d), Blue (b, e), and Green (c, f) filter sets.

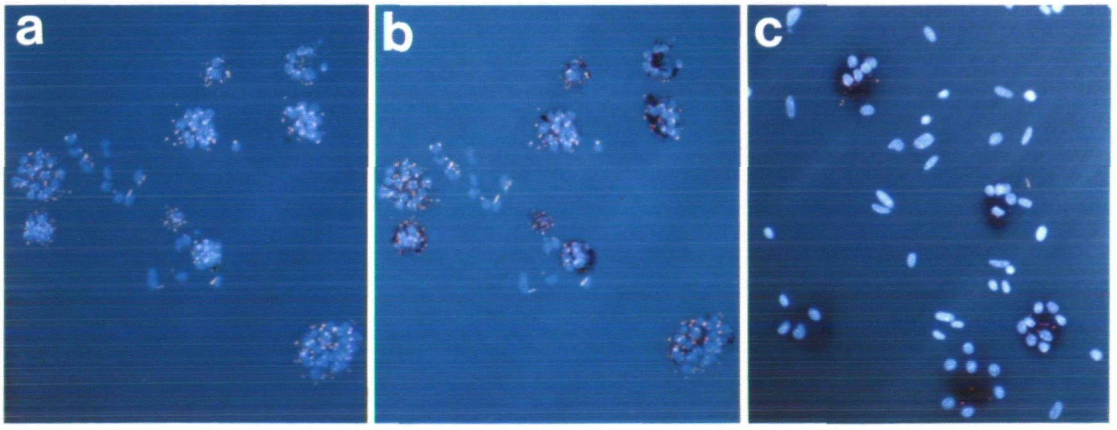

Fig. 2. Relationship between Z-LR-MNA hydrolase activity and TRAPase activity. a: Vital fluorescence staining of rabbit osteoclast-rich cell population with Z-LR-MNA substrate. The proteinase activity was demonstrated as small yellow fluorescent products. Cell nuclei were stained with Hoechst 33258 (blue fluorescence). b: TRAPase staining after the vital fluorescence staining. The TRAPase activity was visualized as the red-purple reaction product. TRAPase-positive multinuclear cells showed intense Z-LR-MNA hydrolase activity, while TRAPase-negative mononuclear cells showed weak activity. c: Mouse osteoclast-like cell double stained for the Z-LR-MNA hydrolase activity and TRAPase activity. Numerous small yellow fluorescent particles were observed in the cell. Cell nuclei were represented by blue fluorescence with Hoechst 33258 staining. The photomicrographs were obtained using UV filter sets.

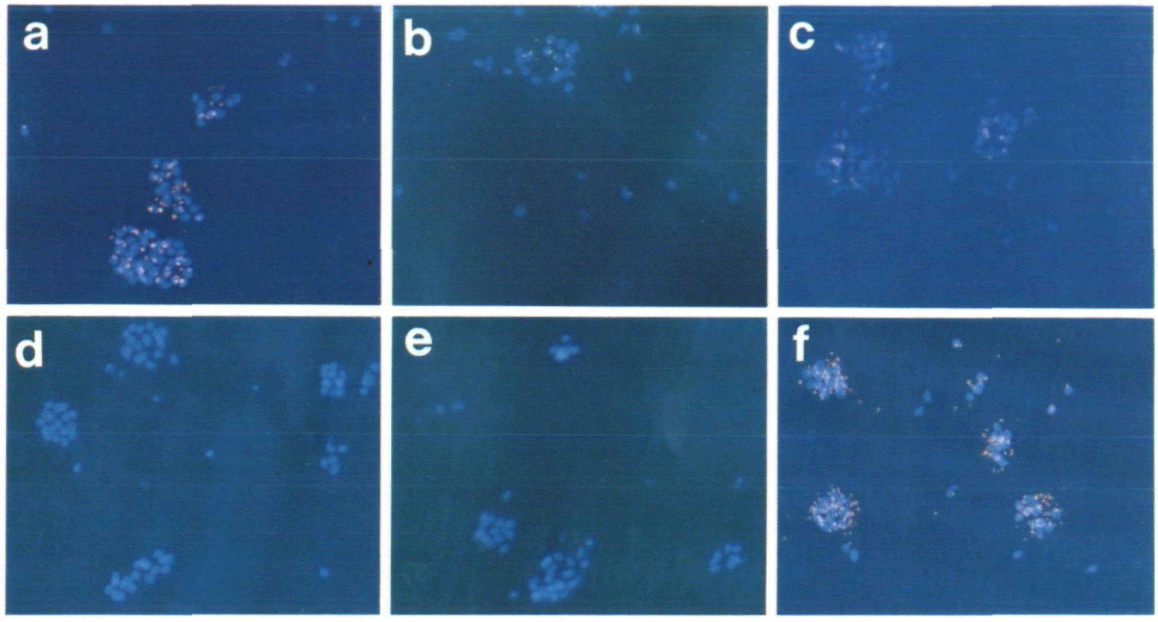

Fig. 3. **Effects of various reagents on Z-LR-MNA hydrolase activity.** As compared with the control cells (a), the activity was markedly diminished in the presence of bafilomycin A1 (b, 1 μM), chloroquine (c, 10 μM), leupeptin (d, 1 μM), and E-64d (e, 1 μM), but not p-APMSF (f, 10 μM). The cells were pretreated with these reagents for 30 min and subjected to the vital fluorescence staining in the presence of the reagents at the same concentrations indicated above. The photomicrographs were obtained using UV filter sets.

while p-APMSF, a serine proteinase inhibitor (Fig. 3f), and pepstatin, an aspartic proteinase inhibitor (data not shown), had no effect on the activity. The same results were obtained in mouse osteoclast-like cells (data not shown). These results suggested that most of the Z-LR-MNA hydrolase activity represented the activity of lysosomal cysteine proteinase(s) in the cells.

We then measured the optimum pH of the Z-LR-MNA hydrolase in osteoclasts, using Z-LR-MCA as the enzyme substrate instead of Z-LR-MNA. The MCA-coupled substrate shows higher solubility in water than that of the MNA-coupled substrate. Moreover, liberated MCA shows about 2.5-fold higher molar fluorescence intensity than that of free MNA. Taking these results into consideration, we decided to use the MCA-coupled substrate in the solution-based *in vitro* assay. We show only the results obtained with the MCA-coupled substrate herein; however, basically the same results were obtained by using the MNA-coupled substrate (data not shown). The total cell extracts were prepared from purified rabbit osteoclasts and mouse osteoclast-like cells (Fig. 4, a and b). In both cell types, the Z-LR-MCA hydrolase activity showed a high single peak at pH between 5.0 and 6.0. When the Z-LR-MCA hydrolase activity was measured at pH 6.0, the specific activity (U/mg cell protein) in the cell extracts of mouse osteoclast-like cells and rabbit osteoclasts was higher than that in mouse calvaria-derived osteoblastic stromal cells and mouse peritoneal macrophages (Table I).

Three-Dimensional Localization of the Z-LR-MNA Hydrolase Activity in Osteoclasts—On the bone surface, resorbing osteoclasts form a tight sealing structure in which bundles of F-actin are accumulated, the so-called actin ring. The osteoclasts secrete protons and lysosomal enzymes unidirectionally onto the bone surface area encircled by the sealing structure (*1, 2, 29*). We examined the three-di-

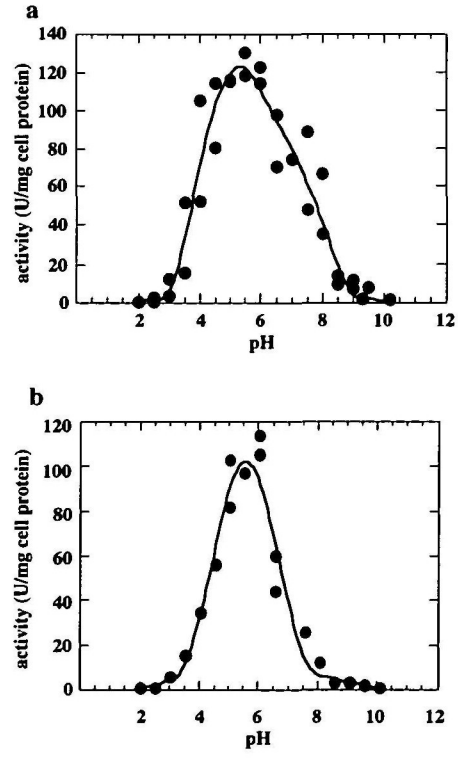

Fig. 4. **Measurement of optimum pH of Z-LR-MCA hydrolase activity in cell extracts of rabbit osteoclasts (a) and mouse osteoclast-like cells (b).** The activity was determined with 5 μM Z-LR-MCA in the presence of 1 mM cysteine and 1 mM EDTA at the pH indicated in the figure. In both rabbit osteoclasts and mouse osteoclast-like cells, the activity was maximal in the acidic pH range from 5.0 to 6.0.

mensional localization of the Z-LR-MNA hydrolase activity in rabbit osteoclasts plated on a dentine disk. The location of the fluorescent products generated by the proteolysis was compared with the position of the actin ring formed by the cells. Figure 5, a-i, shows serial cross-sectional images obtained by confocal microscopy with a 2-μm scanning interval from top to bottom. The actin ring was demonstrated as a red circle (arrow in d, e, and f), and the surface of the dentine was observed as a reddish background. The round black area adjacent to the osteoclast (in e-i) depicts the area resorbed by the cell. The Z-LR-MNA hydrolase activity, visualized as small yellow dots, was found in the intracellular area encircled by the actin ring. The activity was found above the actin ring and also beneath the actin ring, most likely in the bone resorption lacunae.

TABLE I. **Z-LR-MCA hydrolase activity in osteoclasts, osteoblastic stromal cells and macrophages.** The Z-LR-MCA hydrolase activity was determined at pH 6.0 in the presence of 1 mM cysteine and 1 mM EDTA. The cells were lyzed in the buffer containing 1% NP-40 and the supernatant after centrifugation at 15,000×*g* for 30 min was used for the assay as described in "MATERIALS AND METHODS." The results are expressed as the mean±standard deviation (SD) of 3 independent determinations.

Cell type	U/mg cell protein
Rabbit osteoclasts	127.8±15.7
Mouse osteoclast-like cells	111.8±13.0
Mouse calvaria-derived osteoblastic stromal cells	30.9±7.4
Mouse peritoneal macrophage	55.5±9.1

Immunological Analyses for Z-LR-MNA Hydrolase Activity—To examine which cysteine proteinase contributes most to the Z-LR-MNA (or MCA) hydrolase activity, we performed an immunoabsorption experiment using antibodies against cathepsin K and cathepsin L. The total cell extracts of mouse osteoclast-like cells were mixed with the Sepharose CL-4B beads coupled with normal rabbit IgG, anti-CK-C IgG, or anti-CL-C IgG for 8 h at 4 °C, pH 7.0, in the presence of 0.5 mM cysteine. The recovery of Z-LR-MCA hydrolase activity in each flow-through fraction was 90, 35, and 80% for control IgG, anti-CK-C IgG, and anti-CL-C IgG-coupled beads, respectively. About 10% of the activity seemed to be lost during the column manipulation, most likely by non-specific adhesion and spontaneous inactivation of the enzyme. By normalizing each value against that of control IgG-coupled beads, about 60 and 10% of the hydrolase activity were concluded to be absorbed by passing through anti-CK-C and anti-CL-C-coupled beads, respectively (Fig. 6a).

We performed the same immunoabsorption experiment, but using total cell extracts of mouse peritoneal macrophages. The Z-LR-MCA activity in the flow-through fraction of anti-CL-C IgG-coupled beads was 60% of that of

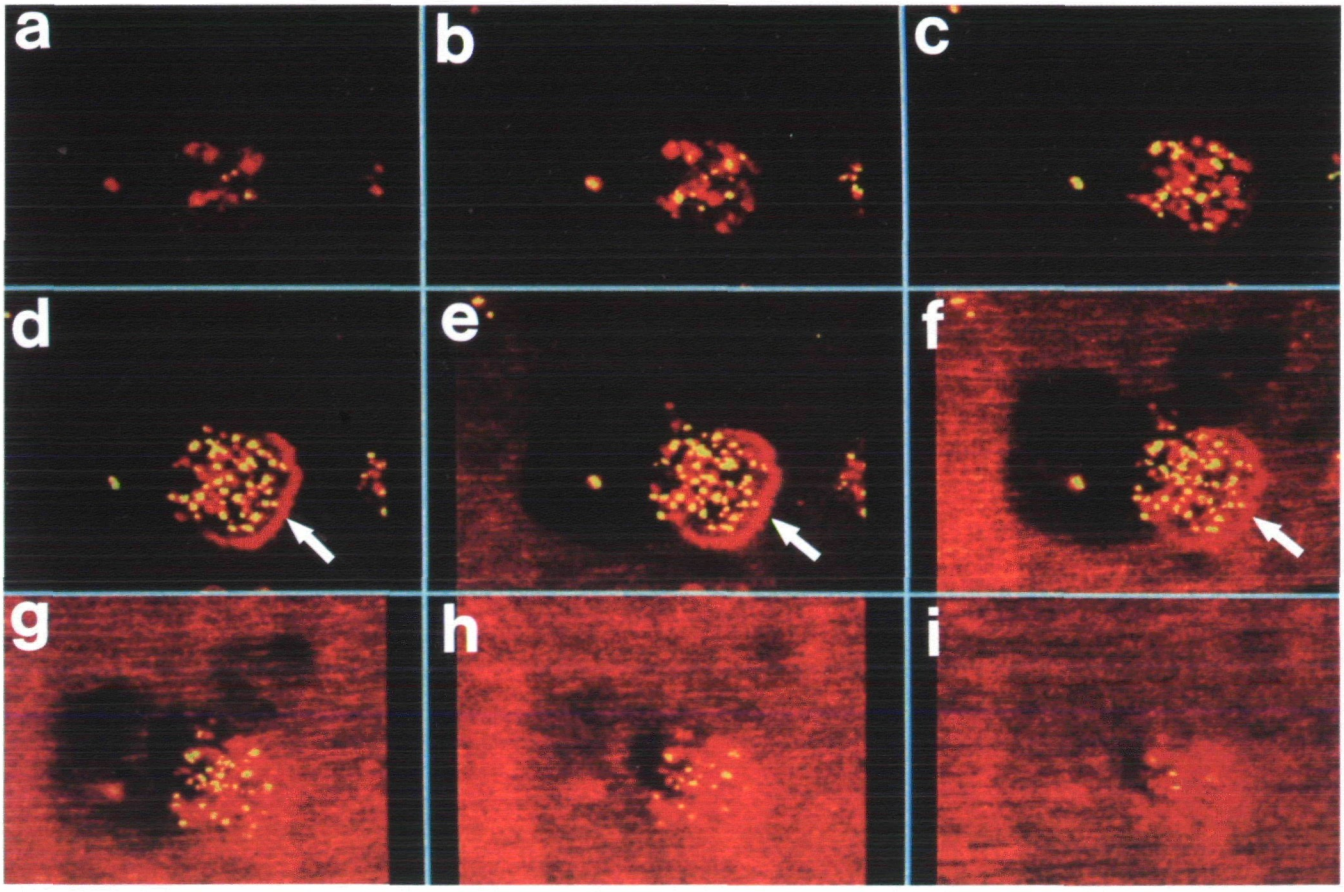

Fig. 5. ***Confocal microscopic observation of the Z-LR-MNA hydrolase activity and the actin ring.*** Rabbit osteoclasts plated on a dentine disk were stained for Z-LR-MNA hydrolase followed by TRITC-phalloidin staining for F-actin. With a confocal microscope, the cells were scanned from top (a) to bottom (i) with a 2-μm scanning interval. The Z-LR-MNA hydrolase activity (yellow particles) was found above and beneath the actin ring (arrow).

control IgG-coupled beads (Fig. 6b). Anti-CK-C IgG-coupled beads caused no apparent reduction of the Z-LR-MCA activity as compared with that of control IgG-coupled beads.

To test the binding efficiency of the IgG-coupled beads we used, the amount of cathepsin K in the flow-through fraction was determined by immunoblotting using anti-CK-C IgG. In the osteoclast lysate, 40 and 27 kDa bands were identified (Fig. 6c, lane 1). Most likely these two bands correspond to the precursor and mature forms of cathepsin K, given the predicted molecular weight of each form (*17, 18*). The two bands completely vanished when the anti-CK-C was pre-incubated with an excess amount of CK-C peptide, but not when it was incubated with CL-C peptide (data not shown). Although the CK-C peptide had about 50% amino acid homology with the CL-C peptide, the anti-CK-C IgG reacted only with CK-C peptide. The efficiency of the column absorption was not 100%, since a small amount of cathepsin K still remained in the flow-through fraction of the anti-CK-C IgG-coupled beads (Fig. 6c, lane 3). The binding efficiency was estimated as approximately 80%, by comparing the band intensity of the flow-through fraction from normal rabbit IgG- and that from anti-CK-C IgG-coupled beads.

In the first experiment on the cell extracts of mouse osteoclast-like cells, cathepsin K was detected only in the adsorbed fraction of anti-CK-C IgG-coupled beads, but not in the adsorbed fractions of other IgG-coupled beads (Fig. 6c, lanes 5-7). In the second experiment on the cell extracts of mouse peritoneal macrophages, cathepsin L was eluted only from anti-CL-C IgG-coupled beads, as shown in Fig. 6c (lane 9). Thus, the anti-CK-C IgG and the anti-CL-C IgG clearly discriminated their antigen protein.

DISCUSSION

Many peptide substrates bearing arylamine derivatives, such as naphthylamine (NA) and MCA, are available for measurement of proteinase activity. However, the NA and MCA liberated by proteolysis are soluble and easily diffuse out of the cells. On the other hand, because MNA forms a fluorescent, insoluble Schiff-base product in the presence of NSA, it is useful for histochemical detection of the proteolytic activity. In these experiments, the reaction product of NSA-coupled MNA showed a wide fluorescence spectrum.

Several previous studies have demonstrated that histochemical staining with Z-Ala-Arg-Arg-MNA is useful for demonstrating the cathepsin B activity in epithelial cells, fibroblasts, and macrophages (*30-35*). Kayser *et al.* have established an automatic method of measurement of cathepsin B activity in a single human thyroid epithelial cell using image analysis and histochemical assay with Z-Ala-Arg-Arg-MNA as the substrate (*36*). Because the bone resorption activity of osteoclasts is greatest when the cells are in contact with stromal cells (*37*), a histochemical method seems to be suitable for examination of the proteinase activities in an individual osteoclast within such mixed cell populations. In initial trials, we tested various protease substrates such as Z-Ala-Arg-Arg-MNA, Z-Arg-Arg-MNA, Z-Gly-Pro-Arg-MNA, and Z-Leu-Arg-MNA for the direct visual detection of the proteinase activities in osteoclasts. We found that Z-Leu-Arg-MNA (Z-LR-MNA) showed the strongest signal in osteoclasts among the substrates we tested. Therefore, we used Z-LR-MNA in the subsequent experiments.

The Z-LR-MNA hydrolase activity in the osteoclasts was apparently higher than that in the mononuclear stromal

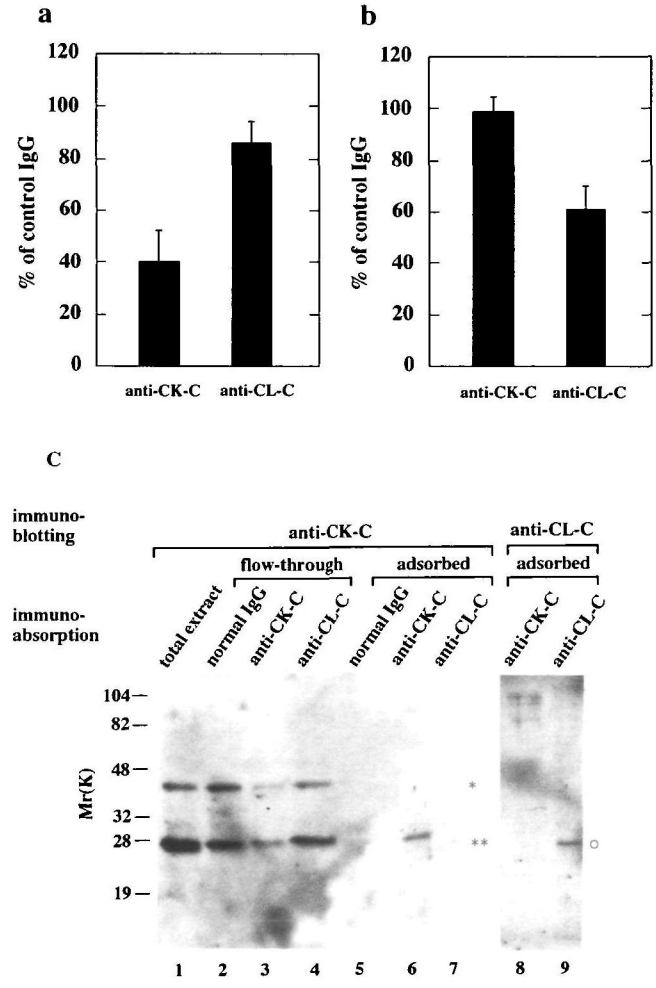

Fig. 6. **Immunological analyses for the Z-LR-MCA hydrolase activity in mouse osteoclast-like cells.** a: Immunoabsorption of the Z-LR-MCA hydrolase activity in mouse osteoclast-like cells by Sepharose CL-4B beads coupled with normal rabbit IgG, anti-cathepsin K (CK-C) IgG, or anti-cathepsin L (CL-C) IgG. The Z-LR-MCA hydrolase activity in the flow-through fraction was measured and normalized against the value obtained for sample treated with the control IgG. The results are expressed as the mean ± SD of 3 separate determinations. b: The same experiment as described in a, but using cell extracts of mouse peritoneal macrophages. The results are expressed as the mean ± SD of 3 separate determinations. c: Immunoblotting analyses. In lanes 1-7, cell extracts of mouse osteoclast-like cells were subjected to immunoabsorption. Total cell extract (lane 1), flow-through fractions of the IgG-coupled Sepharose beads (lanes 2-4), and adsorbed fractions of the IgG-coupled Sepharose beads (lanes 5-7) were detected with anti-CK-C IgG. Cathepsin K was present as the precursor form with an apparent molecular weight of 40 kDa (*) and also as the mature form with a molecular weight of 27 kDa (**). Lanes 8 and 9 show cell extracts of mouse peritoneal macrophages subjected to the immunoabsorption. The adsorbed fraction of anti-CK-C IgG-coupled beads (lane 8) and of anti-CL-C IgG-coupled beads (lane 9) was detected with anti-CL-C antibody. Cathepsin L was observed predominantly as the mature form with an apparent molecular weight of 27 kDa (○ in lane 9). Prestained molecular markers (low range, Bio-Rad Laboratories, Hercules, CA, USA) were used as molecular weight standards.

cells. This observation was in accordance with the higher specific activity of Z-LR-MCA hydrolase in the osteoclast-related cells compared to the osteoblastic stromal cells (Table 1). The Z-LR-MNA hydrolase activity *in situ* was inhibited by bafilomycin A1 and chloroquine treatment. These reagents are known to raise the pH of the acidic cellular compartments such as lysosomes and endosomes (*38*). Therefore, the hydrolysis of Z-LR-MNA apparently occurred in the acidic cellular compartments. Moreover, the maximum hydrolase activity for Z-LR-MCA was obtained in the acidic pH range at around pH 5-6 in both the rabbit osteoclasts and the mouse osteoclast-like cells. The activity was inhibited by cysteine proteinase inhibitors such as leupeptin and E-64d, but not by other classes of proteinases inhibitors. We therefore concluded that the Z-LR-MNA hydrolase activity was derived from lysosomal cysteine proteinase(s).

The localization of the fluorescent product indicates the site of the proteinase activity in the cells. In osteoclasts, the activity was observed throughout the entire cytoplasm and also in close proximity to the bone surface. The staining activity may lead to a better understanding of how the proteinase exerts its function in the cells, in combination with immunohistochemical studies, because staining activity detects only the active mature enzyme, but not the inactive proenzyme which is frequently detected by the immunohistochemical methods. However, one problem in our staining activity procedure arises from the nature of the products of the NSA-coupled MNA: the initial reaction results in the formation of small fluorescent particles within the cells, while, with a higher concentration of the substrate and NSA or with prolonged incubation time, needle-like crystals radiate from the reaction centers and overgrow the outside of the cells. To minimize the crystal overgrowth, we paid special attention to determining the optimum concentrations of the substrate and NSA and also the optimum incubation time.

As lysosomal cysteine proteinases in osteoclasts, cathepsins B, H, K, L, and S have been identified. Any of these cathepsins can hydrolyze Z-LR-MNA, though with different kinetics. Based on the substrate specificities of these enzymes (*19, 20, 39*), cathepsins K, L, and S are thought to be mainly involved in the Z-LR-MNA hydrolase activity in osteoclasts. To examine which proteinases are mainly responsible for the Z-LR-MNA (or MCA) hydrolase activity in osteoclasts, we prepared discriminative antibodies to cathepsins K and L and performed immunological analyses. The specificity of each antibody was verified by means of immunoblotting and immunoabsorption. We observed abundant expression of cathepsin K in both rabbit osteoclasts and mouse osteoclast-like cells, but we detected little cathepsin L in these cells by immunoblotting (data not shown). This is consistent with the observation by Drake *et al.* that the mRNA expression level of cathepsin K is about 100 times higher than that of cathepsin L in human osteoclastoma cells (*16*). In our study, about 60% of the Z-LR-MCA hydrolase activity was immunoabsorbed with antibody against cathepsin K C-terminal peptide. Taking the efficiency of immunoabsorption into consideration, we concluded that, at minimum, more than 60% of the activity in osteoclasts was derived from cathepsin K. The rest of the activity is derived from cathepsin L and also possibly from other enzymes.

The abundant cathepsin K activity in osteoclasts implies a significant role of cathepsin K in bone matrix degradation. Cathepsin K is known to degrade native Type I collagen, the major structural protein component in bone, in the pH range of 5.0-6.0 (*20*). As compared to cathepsin K, a low activity for digestion of native Type I collagen was observed for cathepsins L and S, although these enzymes can digest degenerating collagen (gelatin). Because of the osteoclast-specific expression of cathepsin K (*13, 14, 17*), the matrix protein degradation in the bone resorption process may be distinguished from other types of proteolysis involved in lysosomal cysteine proteinases. We also found that peritoneal macrophages, which are expected to possess a high proteolytic activity, showed no apparent cathepsin K activity.

In this study, we localized the lysosomal cysteine proteinase activity in osteoclasts, by using a substrate with relatively broad specificity, and we found that this activity is mainly due to cathepsin K. Nevertheless, our results would be more definitive, if a specific substrate for cathepsin K were available. The histochemical staining of proteolytic activity seems to be very useful to monitor the activity in a single osteoclast and for analysis of how proteases exert their function in the cells.

REFERENCES

1. Teti, A., Marchisio, P.C., and Zambonin-Zallone, A. (1983) Clear zone in osteoclast function: role of podosomes in regulation of bone-resorbing activity. *Am. J. Physiol.* **261**, C1-C7
2. Baron, R., Neff, L., Brown, W., Courtoy, P.J., Louvard, D., and Farquhar, M.G. (1988) Polarized secretion of lysosomal enzyme: co-distribution of cation-independent mannose-6-phosphate receptors and lysosomal enzymes along the osteoclast exocytic pathway. *J. Cell Biol.* **106**, 1863-1872
3. Delaissé, J.M., Eeckhout, Y., and Vaes, G. (1980) Inhibition of bone resorption in culture by inhibitors of thiol proteinases. *Biochem. J.* **192**, 365-368
4. Delaissé, J.M., Eeckhout, Y., and Vaes, G. (1984) *In vivo* and *in vitro* evidence for the involvement of cysteine proteinases in bone resorption. *Biochem. Biophys. Res. Commun.* **125**, 441-447
5. Delaissé, J.M., Boyde, A., Maconnachie, E., Ali, N.N., Sear, C.H.J., Eeckhout, Y., and Vaes, G. (1987) The effects of inhibitors of cysteine-proteinases and collagenase on the resorptive activity of isolated osteoclasts. *Bone* **8**, 305-313
6. Everts, V., Beertsen, W., and Schröder, R. (1988) Effects of the proteinase inhibitors leupeptin and E-64 on osteoclastic bone resorption. *Calci. Tissue Int.* **43**, 172-178
7. Lerner, U.H. and Grubb, A. (1992) Human cystatin C, a cysteine proteinase inhibitor, inhibits bone resorption in vitro stimulated by parathyroid hormone and parathyroid hormone-related peptide of malignancy. *J. Bone Miner. Res.* **7**, 433-440
8. Kakegawa, H., Nikawa, T., Tagami, K., Kamioka, H., Sumitani, K., Kawata, T., Drobnič-Kosorok, M., Lenarčič, B., Turk, V., and Katunuma, N. (1993) Participation of cathepsin L on bone resorption. *FEBS Lett.* **321**, 247-250
9. Goto, T., Tsukuba, T., Kiyoshima, T., Nishimura, Y., Kato, K., Yamamoto, K., and Tanaka, T. (1993) Immunohistochemical localization of cathepsins B, D and L in the rat osteoclast. *Histochemistry* **99**, 411-414
10. Ohsawa, Y., Nitatori, T., Higuchi, S., Kominami, E., and Uchiyama, Y. (1993) Lysosomal cysteine and aspartic proteinases, acid phosphatase, and an endogenous cysteine proteinase inhibitor, cystatin-β, in rat osteoclasts. *J. Histochem. Cytochem.* **41**, 1075-1083
11. Goto, T., Kiyoshima, T., Moroi, R., Tsukuba, T., Nishimura, Y., Himeno, M., Yamamoto, K., and Tanaka, T. (1994) Localization of cathepsins B, D, and L in the rat osteoclast by immuno-light

and -electron microscopy. *Histochemistry* **101**, 33-40
12. Tezuka, K., Tezuka, Y., Maejima, A., Sato, T., Nemoto, K., Kamioka, H., Hakeda, Y., and Kumegawa, M. (1994) Molecular cloning of a possible cysteine proteinase predominantly expressed in osteoclasts. *J. Biol. Chem.* **269**, 1106-1109
13. Inaoka, T., Bilbe, G., Ishibashi, O., Tezuka, K., Kumegawa, M., and Kokubo, T. (1995) Molecular cloning of human cDNA for cathepsin K: novel cysteine proteinase predominantly expressed in bone. *Biochem. Biophys. Res. Commun.* **206**, 89-96
14. Brömme, D. and Okamoto, K. (1995) Human cathepsin O2, a novel cysteine protease highly expressed in osteoclastomas and ovary molecular cloning, sequencing and tissue distribution. *Biol. Chem. Hoppe-Seyler* **376**, 379-384
15. Li, Y-P., Alexander, M., Wucherpfenning, A.L., Yelick, P., Chen, W., and Stashenko, P. (1995) Cloning and complete coding sequence of a novel human cathepsin expressed in giant cells of osteoclastomas. *J. Bone Miner. Res.* **10**, 1197-1202
16. Drake, F.H., Dodds, R.A., James, I.E., Connor, J.R., Debouck, C., Richardson, S., Lee-Rykaczewski, E., Coleman, L., Rieman, D., Barthlow, R., Hastings, G., and Gowen, M. (1996) Cathepsin K, but not cathepsins B, L, or S, is abundantly expressed in human osteoclasts. *J. Biol. Chem.* **271**, 12511-12516
17. Rantakokko, J., Aro, H.T., Savontaus, M., and Vuorio, E. (1996) Mouse cathepsin K: cDNA cloning and predominant expression of the gene in osteoclasts, and in some hypertrophying chondrocytes during mouse development. *FEBS Lett.* **393**, 307-313
18. Gelb, B.D., Moissoglu, K., Zhang, J., Martignetti, J.A., Brömme, D., and Desnick, R.J. (1996) Cathepsin K: isolation and characterization of the murine cDNA and genomic sequence, the homologue of the human pycnodysostosis gene. *Biochem. Mol. Med.* **59**, 200-206
19. Bossard, M.J., Tomaszek, T.A., Thompson, S.K., Amegadzie, B.Y., Hanning, C.R., Jones, C., Kurdyla, J.T., McNulty, D.E., Darke, F.H., Gowen, M., and Levy, M.A. (1996) Proteolytic activity of human osteoclast cathepsin K. Expression, purification, activation, and substrate identification. *J. Biol. Chem.* **271**, 12517-12524
20. Brömme, D., Okamoto, K., Wang, B.B., and Biroc, S. (1996) Human cathepsin O2, a matrix protein-degrading cysteine protease expressed in osteoclasts. Functional expression of human cathepsin O2 in *Spodoptera frugiperda* and characterization of the enzyme. *J. Biol. Chem.* **271**, 2126-2132
21. Inui, T., Ishibashi, O., Inaoka, T., Inaoka, T., Origane, Y., Kumegawa, M., Kokubo, T., and Yamamura, T. (1997) Cathepsin K antisense oligodeoxynucleotide inhibits osteoclastic bone resorption. *J. Biol. Chem.* **272**, 8109-8112
22. Littlewood, E.A., Kokubo, T., Ishibashi, O., Inaoka, T., Wlodarski, B., Gallagher, J.A., and Bilbe, G. (1997) Localization of cathepsin K in human osteoclasts by *in situ* hybridization and immunohistochemistry. *Bone* **20**, 81-86
23. Tezuka, K., Sato, T., Kamioka, H., Nijweide, P.J., Tanaka, K., Matsuo, T., Ohta, M., Kurihara, N., Hakeda, Y., and Kumegawa, M. (1992) Identification of osteopontin in isolated rabbit osteoclasts. *Biochem. Biophys. Res. Commun.* **186**, 911-917
24. Takahashi, N., Akatsu, T., Udagawa, N., Sasaki, T., Yamaguchi, A., Moseley, J.M., Martin, T.J., and Suda, T. (1988) Osteoblastic cells are involved in osteoclast formation. *Endocrinology* **123**, 2600-2602
25. Hashimoto, F., Kobayashi, Y., Miyazaki, Y., Kamiya, T., Mataki, S., Kobayashi, K., Kato, Y., and Sakai, H. (1997) Antigenicity of pro-osteocalcin in hard tissue: the authenticity to visualize osteocalcin-producing cells. *J. Bone Miner. Metab.* **15**, 122-131
26. Joseph, L.J., Chang, L.C., Stamenkovich, D., and Sukhatme, V.P. (1988) Complete nucleotide and deduced amino acid sequences of human and murine preprocathepsin L. An abundant transcript induced by transformation of fibroblasts. *J. Clin. Invest.* **81**, 1621-1629
27. Yoshimori, T., Semba, T., Takemoto, H., Akagi, S., Yamamoto, A., and Tashiro, Y. (1990) Protein disulfide-isomerase in rat exocrine pancreatic cells is exported from the endoplasmic reticulum despite possessing the retention signal. *J. Biol. Chem.* **265**, 15984-15990
28. Lowry, O.H., Rosebrough, N.J., Farr, A.L., and Randall, R.J. (1951) Protein measurement with the folin phenol reagent. *J. Biol. Chem.* **193**, 265-275
29. Väänänen, H.K. and Horton, M. (1995) The osteoclast clear zone is a specialized cell-extracellular matrix adhesion structure. *J. Cell Sci.* **108**, 2729-2732
30. Dolbeare, F.A. and Smith, R.E. (1977) Flow cytometric measurement of peptidases with use of 5-nitrosalicylaldehyde and 4-methoxy-β-naphthylamine derivatives. *Clin. Chem.* **23**, 1485-1491
31. Graf, M., Leemann, U., Ruch, F., and Sträuli, P. (1979) The fluorescence and bright field microscopic demonstration of cathepsin B in human fibroblasts. *Histochemistry* **64**, 319-322
32. Dolbeare, F. and Vanderlaan, M. (1979) A fluorescent assay of proteinases in cultured mammalian cells. *J. Histochem. Cytochem.* **27**, 1493-1495
33. van Noorden, C.J.F., Vogels, I.M.C., Everts, V., and Beertsen, W. (1987) Localization of cathepsin B activity in fibroblasts and chondrocytes by continuous monitoring of the formation of a final fluorescent reaction product using 5-nitrosalicylaldehyde. *Histochem. J.* **19**, 483-487
34. Sakai, K., Nii, Y., Ueyama, A., and Kishino, Y. (1991) Fluorescence demonstration of cathepsin B activity in fractionated alveolar macrophages. *Cell. Mol. Biol.* **37**, 353-358
35. Reddy, V.Y., Zhang, Q-Y., and Weiss, S.J. (1995) Pericellular mobilization of the tissue-destructive cysteine proteinases, cathepsins B, L, and S, by human monocyte-derived macrophages. *Proc. Natl. Acad. Sci. USA* **92**, 3849-3853
36. Kayser, L., Perrild, H., Thomsen, J., and Høyer, P.E. (1996) Microfluorometric kinetic analysis of cathepsin B activity in single human thyroid follicular epithelial cells using image analysis and continuous monitoring. *Histochem. J.* **28**, 257-263
37. Jimi, E., Nakamura, I., Amano, H., Taguchi, Y., Tsurukai, T., Tamura, M., Takahashi, N., and Suda, T. (1996) Osteoclast function is activated by osteoblastic cells through a mechanism involving cell-to-cell contact. *Endocrinology* **137**, 2187-2190
38. Yoshimori, T., Yamamoto, A., Moriyama, Y., Futai, M., and Tashiro, Y. (1991) Bafilomycin A1, a specific inhibitor for vacuolar-type H^+-ATPase, inhibits acidification and protein degradation in lysosomes of cultured cells. *J. Biol. Chem.* **266**, 17707-17712
39. Aibe, K., Yazawa, H., Abe, K., Teramura, K., Kumegawa, M., Kawashima, H., and Honda, K. (1996) Substrate specificity of recombinant osteoclast-specific cathepsin K from rabbits. *Biol. Pharm. Bull.* **19**, 1026-1031
40. Kakudo, S., Miyazawa, K., Kameda, T., Mano, H., Mori, Y., Yuasa,T., Nakamaru, Y., Shiokawa, M., Nagahira, K., Tokunaga, S., Hakeda, Y., and Kumegawa, M. (1996) Isolation of highly enriched rabbit osteoclasts from collagen gels: A new assay system for bone-resorbing activity of mature osteoclasts. *J. Bone Miner. Metab.* **14**, 129-136